Chapter 2

Evaluation of a Regional Climate Model for the Upper Blue Nile Region

Tadesse Terefe Zeleke, Baylie Damtie Yeshita and Fentahun Muluneh Agidew

Additional information is available at the end of the chapter

http://dx.doi.org/10.5772/64954

Abstract

The fourth version of the International Center for Theoretical Physics (ICTP) Regional Climate Model (RegCM4) model is evaluated for its performance over Upper Blue Nile River Basin Region (UBNRBR). The model rainfall captured the observed spatial and temporal variability of rainfall over the basin during the spring (MAM) and summer (JJA) seasons. The simulation dataset is generated using the RegCM4 for the period 1982–2009. The UBNRBR is first divided into 14 homogeneous regions using criteria including Rotated Empirical Orthogonal Function (REOF), spatial correlation and topographical features. Spatially averaged observed and simulated rainfall time series are then generated and analyzed for each region. Standardized rainfall anomalies of the observations and the simulated data are highly correlated over most of central regions, while a weak correlation is found over the east border regions of the basin. The dominant modes of rainfall variability are identified using REOF. The first leading patterns of rainfall and upper wind (averaged between 100 and 300 hpa) are highly correlated and exhibit similar features between simulated and observed dataset over the basin. Similarly, the first loading pattern of low level wind (averaged between 850 and 1000 hpa) exhibits a dipole structure across the southwestern and southeastern regions of the UBNRBR. The correlations with significant rotated principal components (RPCs) across gridded gauge, and model rainfall fields with that of low- and upper level winds show the presence of significant relationship (correlation exceeding ~0.6). Overall, that the RegCM4 shows a good performance in simulating the spatial and temporal variability of precipitation over UBNRBR.

Keywords: RegCMx, variability, RPC, Upper Blue Nile River Basin Region (UBNRBR)

1. Introduction

Regional climate models (RCMs) have become increasingly important tools to downscale global (large scale) climate information for regional applications. Numbers of studies have demonstrated the capability of regional climate models of different version (RegCMx) in downscaling global climate information for regional applications and representing details of regional climate [1–8]. Such models are driven by initial and lateral boundary conditions taken from reanalysis, observations and from global circulation model (GCM) output [3–5, 9–13]. RCMs become suitable tools for regional process studies, which increase our understanding about influence of local climatic forcing superimposed on large-scale climate variability. By coupling appropriate land surface, hydrologic or lake models with that of RCMs enables accurate simulation of detailed precipitation, temperature, surface hydrological features and other meteorological variables [14].

The sensitivity of RegCMx to dynamical configuration such as domain size, resolution and the physical parameterizations has been demonstrated in a number of studies [1, 4, 5, 11, 13]. Hence, before applying a regional climate model for regional climate variability studies, the accuracy of the model in reproducing the observed regional climate should be assessed to establish its strengths and weaknesses for the specific region [3].

Regional climate models have been utilized extensively for mid-latitude regions in wide-ranging surface climate and hydrologic process investigations. Sensitivity studies and simulation of present, past and future climate on the mesoscale and regional scale have been carried out [2, 3, 7, 11, 12, 15, 16]. Relatively few studies exist for eastern Africa climate [4, 5, 8, 17–19]. Most of the above studies of eastern Africa [except 18, 19] focused on the spring and autumn seasons, as these are the main and short rainy seasons for the equatorial Africa. The performance of the RegCM3 in reproducing the Ethiopian summer rainfall variability also evaluated [18, 19]. They found that RegCM3 not only reproduced the spatial variability of dry and wet years but also correlated well with gauge data.

Based on these considerations, in this chapter, the performance of a regional climate model (an updated version of the RegCM4) is presented [20]. Here, we briefly discuss/compare the essential atmospheric variables of observational and/with model simulation that will be necessary in the rest of the chapter to understand the various characteristics of rainfall in the basin. Such as in representing the climatology, inter/intra annual variability of atmospheric variables including rainfall and wind field with respect to relatively large set of rain gauge and satellite based observations and reanalysis datasets.

2. Model, data and methodology

2.1. Model description

The regional climate model used in this study is the ICTP RegCM4 described by Giorgi et al. [20]. It is a hydrostatic model based on the dynamical core of the Penn State/NCAR Mesoscale

http://dx.doi.org/10.5772/64954

Model version 4 [21] with the developments described by Giorgi et al. [11, 12]. RegCM4 includes a range of physics options, and for the present work, it uses the radiation scheme of Community Climate Model version 3 (CCM3) [22], the nonlocal planetary boundary layer scheme originally developed by Holtslag et al. [23] and later modified as described by Giorgi et al. [11, 20]. The Biosphere–Atmosphere Transfer Scheme in [24] is used for land surface process calculations. Precipitation is represented by two different terms: resolvable (large-scale non-convective) and convective (subgrid-cumulus). The resolvable scale precipitation is represented by the subgrid explicit moisture scheme [25]. For convective precipitation, three options are available: (1) the modified Anthes-Kuo scheme [12, 26], (2) the Grell scheme [21] and (3) the Emanuel scheme [27]. In addition, different schemes can be chosen for land and ocean regions [20]. After many preliminary tests, we selected the Grell scheme with the Fritsch-Chappel closure [11, 12, 28] over land and the Emanuel scheme over the ocean grid points. More information on the different physics schemes and applications of the RegCM4 model system can be found in the study of Giorgi et al. [20].

2.1.1. Experimental setup

The simulation/analysis period is 1982–2009, and we applied similar experimental setup with previous study; in which, its initial and lateral boundary conditions are obtained from the new ERA-Interim 1.5° × 1.5° third generation ECMWF gridded reanalysis product [29]. The sea surface temperature (SST) used to force RegCM4 is obtained from the National Oceanic and Atmospheric Administration (NOAA) weekly optimum interpolation (wk-OI) [30] on one-degree grid. The 10-min resolution global land cover characterization (GLCC) dataset for vegetation cover, land use and elevation is used as obtained from the United States Geological Survey (USGS). The model domain (**Figure 1**), the upper right panel, covers most of the African

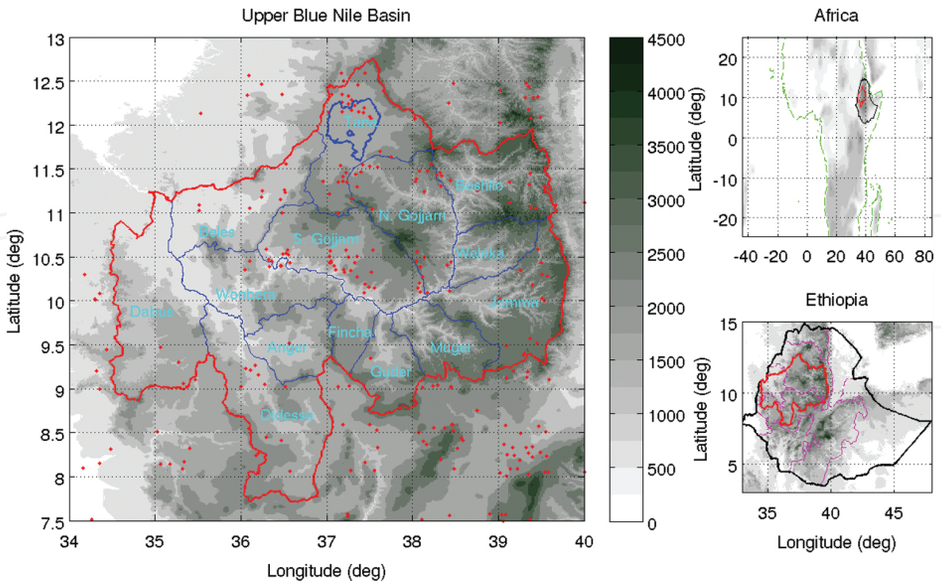

Figure 1. Topography (in meters) of the study area. The blue lines are the 14 homogeneous rainfall regions. The red dots represent the rainfall stations used in this study.

continent and adjacent ocean waters at a grid point spacing of 50 km [31]. This study showed that this domain size is sufficient to obtain a realistic simulation of the climate of UBNRBR.

2.2. Data

The station rainfall dataset used to calibrate the model output is obtained from the Ethiopian National meteorological Agency (EMA). It includes 430 unevenly distributed stations throughout the region for the period 1979–2014. The distribution of the gauges and quality control methods for the observed rainfall dataset are discussed in detail [31]. In addition to the station data described above, we use a blended gauge and satellite product: the global precipitation climatology project (GPCP) described by Adler et al. [32]. The SST is obtained from the UK Met Office Global Sea Ice and Sea Surface Temperature (HadISST2) described by Rayner et al. [33]. This product includes SST observations and satellite-derived estimates at the monthly scale with a resolution of 1° × 1°. The third generation European Centre for Medium-Range Weather Forecasts (ECMWF) 1.5° × 1.5° gridded reanalysis product of ERA-Interim [29] and National Centers for Environmental Prediction-National Center for Atmospheric Research (NCEP–NCAR) reanalysis products are also used [34].

2.3. Data analysis methods

To capture the patterns of co-variability of rainfall and other atmospheric variables at different stations and in the Upper Blue Nile Region, the principal component (PC) analysis (PCA) is applied to the time series. The method consists of computing the covariance matrix of the analyzed atmospheric variable dataset with the corresponding eigenvalues and eigenvectors [35]. The projection of the analyzed atmospheric fields (e.g., rainfall, wind, etc.) into the orthonormal eigenfunctions provides the PC score time series. The spatial patterns (eigenvectors), properly normalized (divided by their Euclidean norm and multiplied by the square root of the corresponding eigenvalues), are called empirical orthogonal function (EOF) or simply "loadings." The loadings in this study are the correlation values between the original data time series at each grid point and the corresponding principal component time series.

In order to extract more localized spatial patterns of variability, we apply the varimax rotation to the loadings [36–39]. Rotated empirical orthogonal function (REOF) analysis is applied to atmospheric variables such as rainfall, low-level wind (averaged between 850 and 1000 hPa), upper level wind (average of pressure levels between 100 and 300 hPa), vertical wind profile averaged over the longitude band between 35°W and 68°E and for selected oceanic basins. The region that is included in the REOF analysis of rainfall is between 34° and 40°E and 7.5° and 13°N for consistency with the gauge data.

To remove the influences of location and spread from a set of data, all atmospheric variables time series are standardized by subtracting the mean and dividing by the standard deviation. For each mode, a spatial pattern of loadings describes its area of influence and time scores that reveal the amplitude and wavelength of oscillation. Hence, we used standardized anomalies of time scores (PCs/RPCs) for correlation analysis of the dominant modes of atmospheric variables.

http://dx.doi.org/10.5772/64954

3. Result and discussion

3.1. Characteristics of large-scale circulation

Spring season climatological patterns of both ERA-Interim and model simulation upper level horizontal wind (**Figure 2a**, **2b** and **2e**) shows strong spatial consistency. The pattern corresponds to an anomalous southerly extension of subtropical westerly jet streams (STWJ) over northern Africa is reproduced very well by RegCM4.

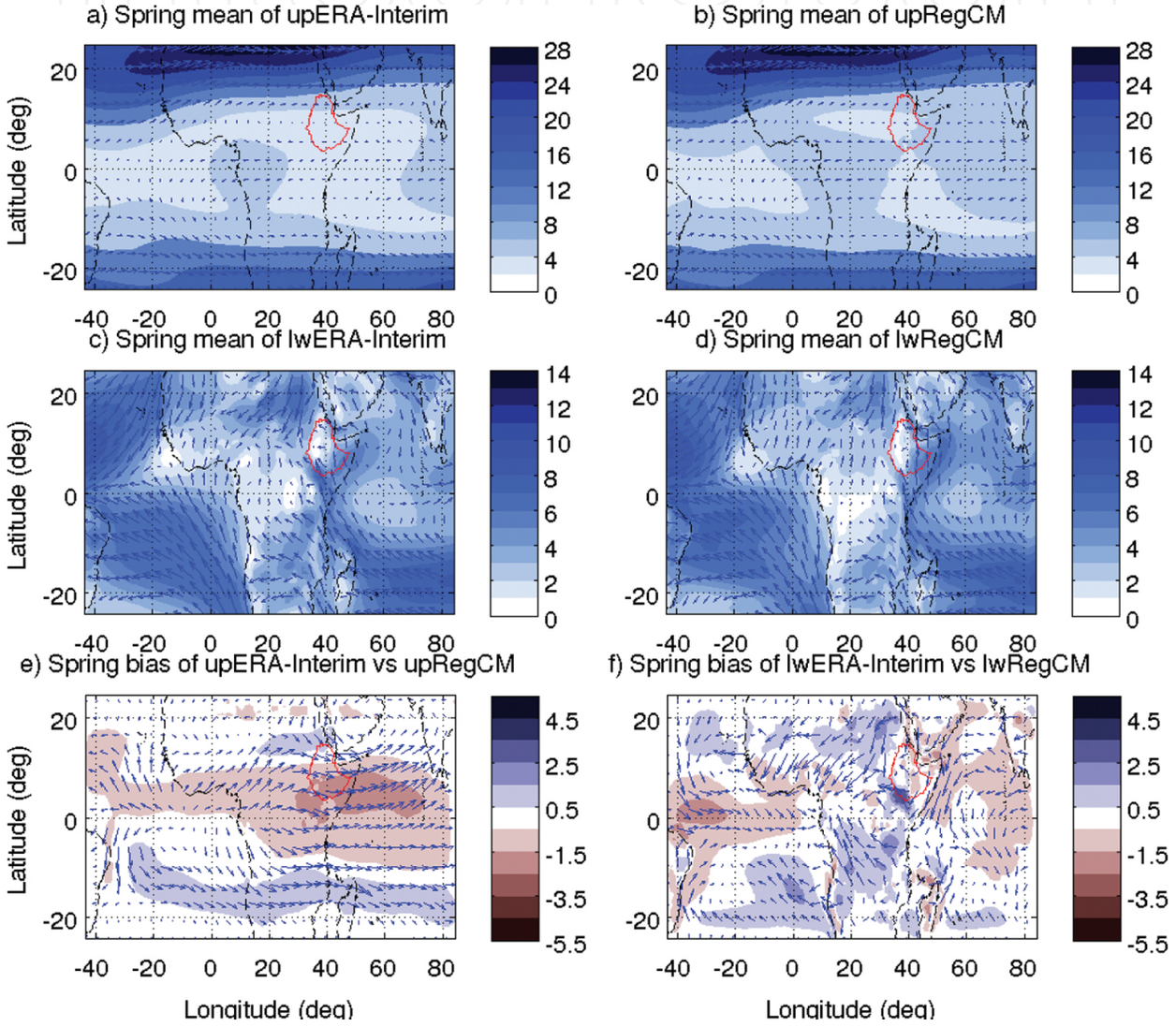

Figure 2. Spring (MAM) season mean horizontal wind: (a) ERA-Interim upper level (averaged between 100 and 300 hPa) wind, (b) RegCM4 upper level wind, (c) ERA-Interim low-level (averaged between 850 and 1000 hPa) wind, (d) RegCM4 low-level wind, (e) the bias of upper wind ERA-Interim vs. RegCM4 and (f) the bias of lower wind ERA-Interim vs. RegCM4.

This pattern in both ERA-Interim and model shows relatively narrow and shallow streams with maximum wind speed. The downward bent of subtropical westerly jet stream is related

to a large-scale convection in the lower troposphere, which is conducive condition for spring rain getting regions of Ethiopia [19, 40]. The STWJ is formed as a result of conservation of angular momentum as the air moves from the lower latitudes to the higher latitudes [19 and reference there in]. The low-level horizontal wind climatology for the spring season in ERA-Interim and RegCM4 simulation (**Figure 2c**, **2d** and **2f**) shows a good agreement in both the magnitude and direction.

Similar, comparison of summer ERA-Interim and RegCM4 horizontal upper level winds indicates a strong similarity (**Figure 3a**, **3b** and **3e**) in representing the location and strength of the tropical easterly jet (TEJ) core, even though the jet stream is slightly stronger in the model over regions south of Chad, Central African Republic, central and eastern Ethiopia. The TEJ extends from southeast Asia across the Indian Ocean towards northeast Africa, with the jet core positioned above 10°N over the Arabian Peninsula and eastern Africa, and tilted southward over central and western Africa. The low-level wind climatology for the summer season in ERA-Interim and RegCM4 is shown in **Figure 3c**, **3d** and **3f**. Like spring, summer season also showed a good agreement in both the magnitude and direction of the east African low-level jet (EALLJ).

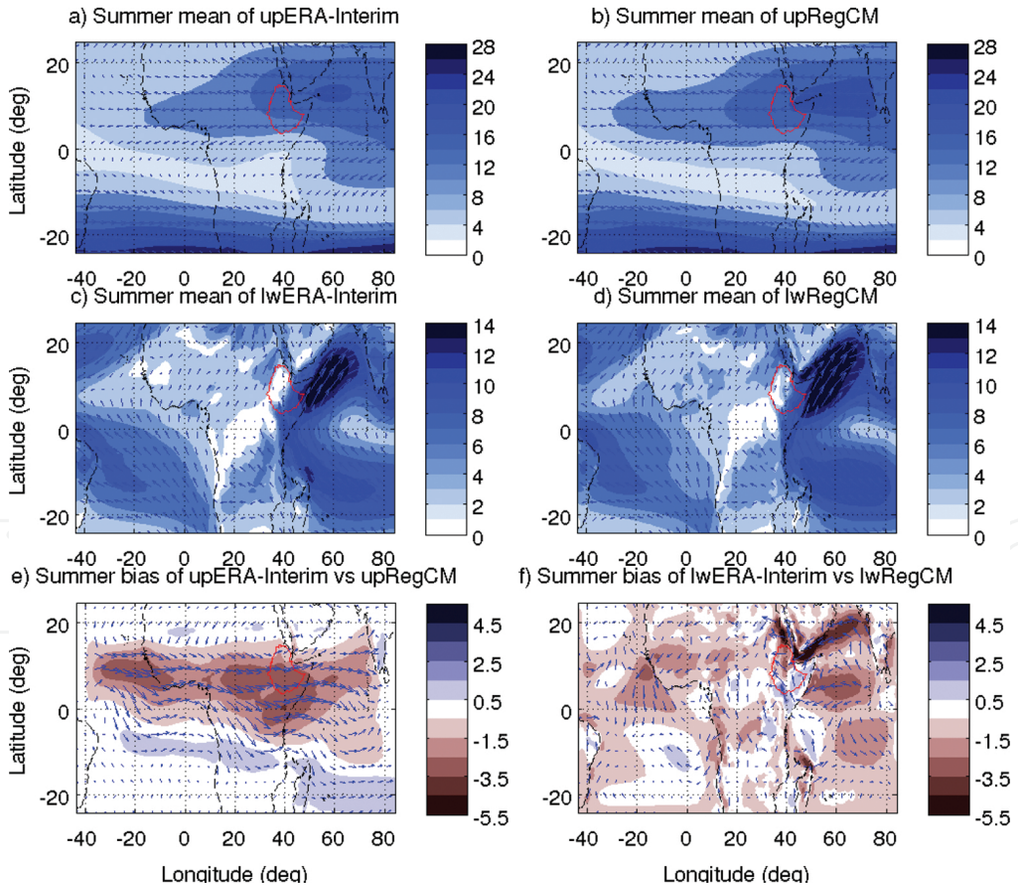

Figure 3. Summer (JJA) season mean horizontal wind: (a) ERA-Interim upper level wind, (b) RegCM4 upper level wind, (c) ERA-Interim low-level wind, (d) RegCM4 low-level wind, (e) the bias of upper wind ERA-Interim vs. RegCM and (f) the bias of lower wind ERA-Interim vs. RegCM.

http://dx.doi.org/10.5772/64954

The correlation with the time series of the wind field and the first rotated principal component (RPC1) of the upper level wind (**Figure 4a** and **4b**) reveals that the spatial pattern of the dominant mode of variability at upper levels is a dipole structure, which shows positive above ~10°N and negative below ~10°N in both model and ERA-Interim. The boundary of the dipole pattern in the model is shifted slightly northward and has stronger magnitude over southern regions.

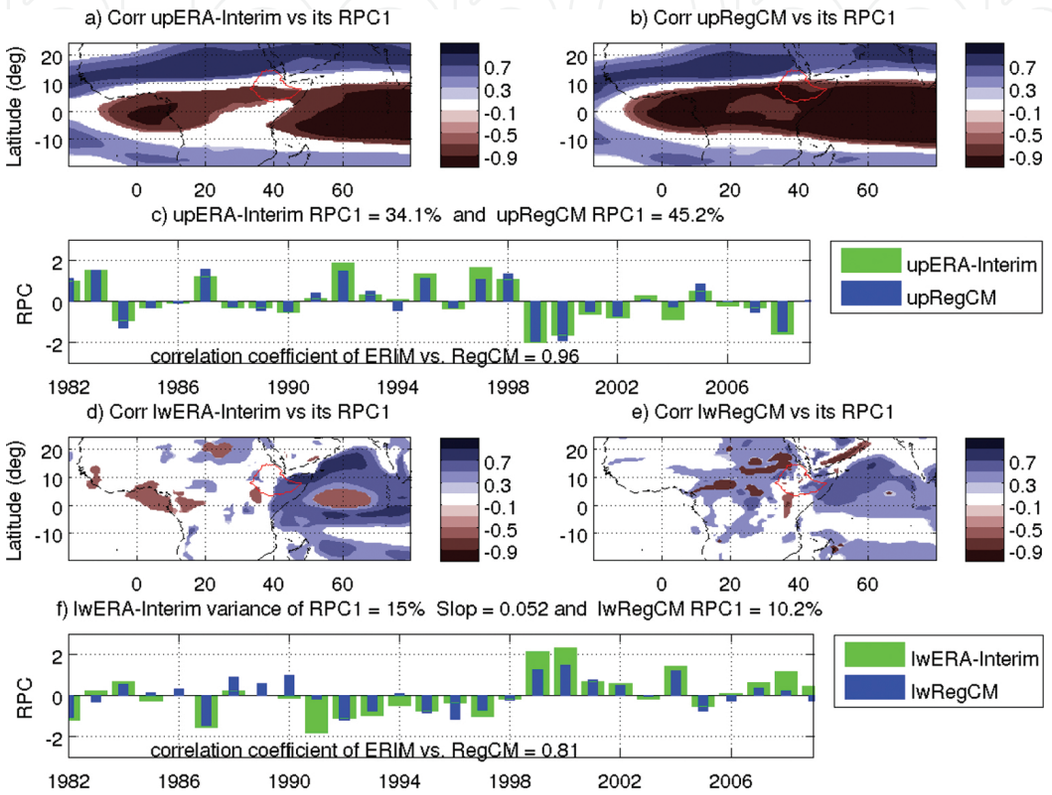

Figure 4. Spring (MAM) season: (a) correlation patterns of upper level horizontal ERA-Interim wind vs its dominant RPC1, (b) correlation patterns of upper level horizontal RegCM wind vs its dominant RPC1, (c) dominant time evolutions of upper level wind ERA-Interim and RegCM, (d) correlation patterns of low level horizontal ERA-Interim wind vs its dominant RPC1, (e) correlation patterns of low level horizontal RegCM wind vs its dominant RPC1 and (f) dominant time evolutions of low level wind ERA-Interim and RegCM.

The variance explained by the first RPC of the model (~45%) and ERA-Interim (~34%) are more than 1/3 of total variance. The intra-annual variability of RPC1 in ERA-Interim and RegCM4 (**Figure 4c**) shows a good agreement (correlation value of ~0.96) and the extreme years (1982/83, 1984, 1992, 1997–2000, 2008) are well captured. The similarity of variability of low-level horizontal wind patterns in **Figure 4d** and **4e** describes the performance of the model in representing the region of dominant variability in the wind field, which explains ~15% and ~10% of total variance, respectively, although small difference are observed over southwest regions of Ethiopia. Significant and high correlation (correlation value of ~0.81) of the dominant time components (RPC1s, **Figure 4f**) confirms the ability of the model to simulate the large-scale circulation. The importance/link of variability of this wind in its magnitude and direction to the Upper Blue Nile River Basin climate is discussed detail in the next Section.

Like spring, during summer season quit similar correlation (upper level wind field and its first RPC1) patterns of (**Figure 5a** and **5b**) ERA-Interim and RegCM are observed, which describes the characteristics of TEJ in both reanalysis and model simulation. The fractions of variance explained by these patterns are ~46% and 51% of ERA-Interim and RegCM, respectively. The time evolutions (RPC1s) of ERA-Interim and RegCM (**Figure 5c**) shows a good agreement (correlation value of ~0.95), and in particular, the extreme negative years (1983, 1987, 1997 and 2009) and positive years (1988, 1994 and 1998) are well captured.

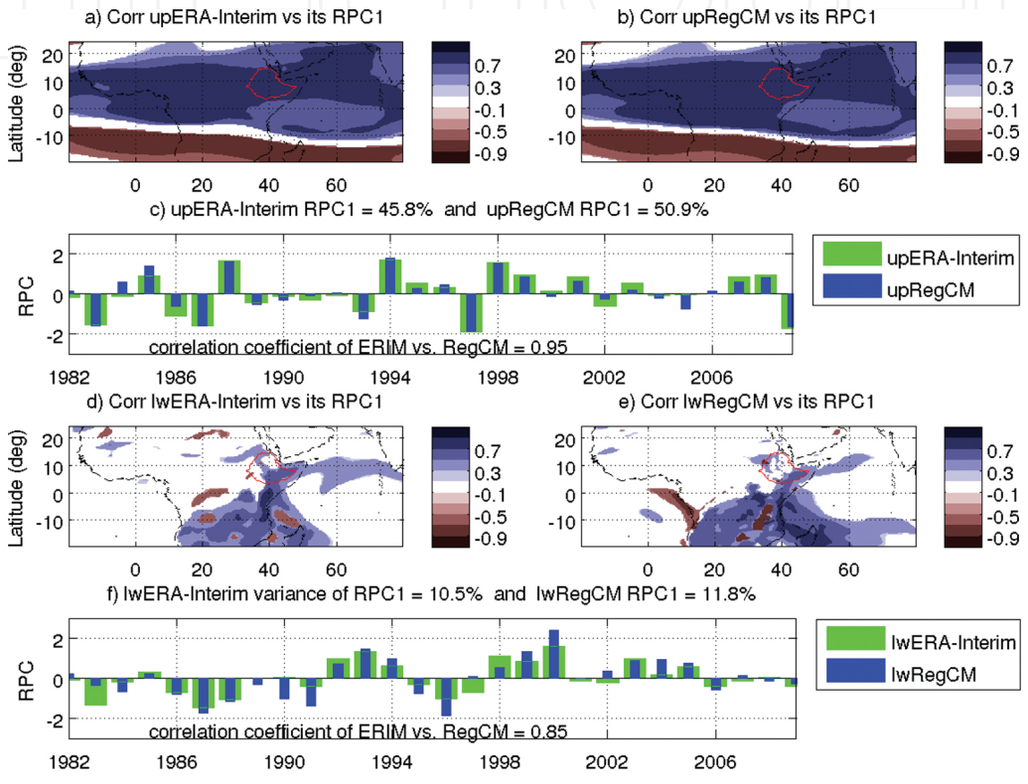

Figure 5. Summer (JJA) season: (a) correlation patterns of upper level horizontal ERA-Interim wind vs its dominant RPC1, (b) correlation patterns of upper level horizontal RegCM wind vs its dominant RPC1, (c) dominant time evolutions of upper level wind ERA-Interim and RegCM, (d) correlation patterns of low level horizontal ERA-Interim wind vs its dominant RPC1, (e) correlation patterns of low level horizontal RegCM wind vs its dominant RPC1 and (f) dominant time evolutions of low level wind ERA-Interim and RegCM.

The patterns of the dominant mode of variability in the lower level wind of the ERA-Interim reanalysis and RegCM4 are essentially identical (**Figure 5d** and **5e**) and show a positive loading over coast of Somalia, which corresponds to east African low-level jet (EALLJ). **Figure 5f** shows the variances explained by the first RPC of the reanalysis and models are ~11 and 12%, respectively. The correlation between the low-level ERA-Interim and RegCM4 wind is ~0.85, which shows the resemblance of the two time series (**Figure 5f**).

3.2. Rainfall climatology, annual cycle, and intra-annual variability

In this section, we analyze the spatial patterns, annual cycle and intra-annual variability of spring and summer rainfall over Upper Blue Nile Region. Mean seasonal rainfall over the

http://dx.doi.org/10.5772/64954

region for the period 1982–2009 shows that the southern and central mountainous regions receive on average more than 12 mm/day during summer and small (1–2 mm/day) amount of rainfall during spring seasons (**Figure 6**). The western and eastern regions, which are semiarid, receive comparably less precipitation during these seasons. The model reproduces reasonably well this climatological pattern of rainfall, although with positive and negative biases over the western mountainous regions and some isolated areas of Upper Blue Nile River Basin region. It exhibits also a central-east/west gradient where rainfall decreases from ~12 to less than ~7 mm/day. RegCM4 forced by ERA-Interim reanalysis capture the location of higher precipitation rates in the southwest, central and northeastern region better than GPCP and CRU dataset. We also note that the GPCP dataset show relatively low precipitation amounts over the southern and central mountain regions of the basin with respect to gauge.

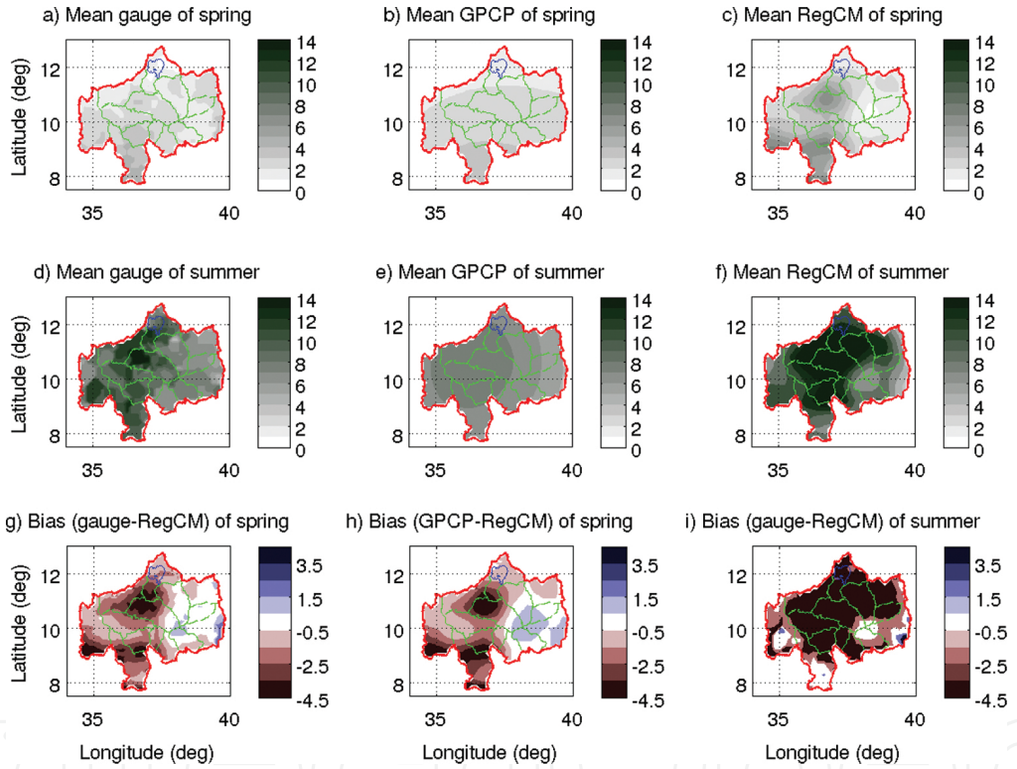

Figure 6. Rainfall: (a) spring mean gauge rainfall, (b) spring GPCP mean rainfall, (c) spring RegCM mean rainfall, (d) summer mean gauge rainfall, (e) summer GPCP mean rainfall, (f) summer RegCM mean rainfall, (g) bias of gauge vs. RegCM during spring, (h) bias of GPCP vs RegCM during spring and (i) bias of gauge vs. RegCM during summer.

Figure 7 shows the mean annual cycle for the homogeneous rainfall regions of the basin using different sets of observations (gauge, GPCP and CRU) and RegCM4 simulation. The annual cycle values are averaged for each homogeneous region of the Upper Blue Nile River Basin over the whole observation and simulation periods. Over Tana subregions (**Figure 7a**), which lie over the "Semien Mountain," the model captures the summer monsoon rainfall and the pre- (May) and post-monsoon rain, although some slight differences in the intensities among the observed and model estimates are observed.

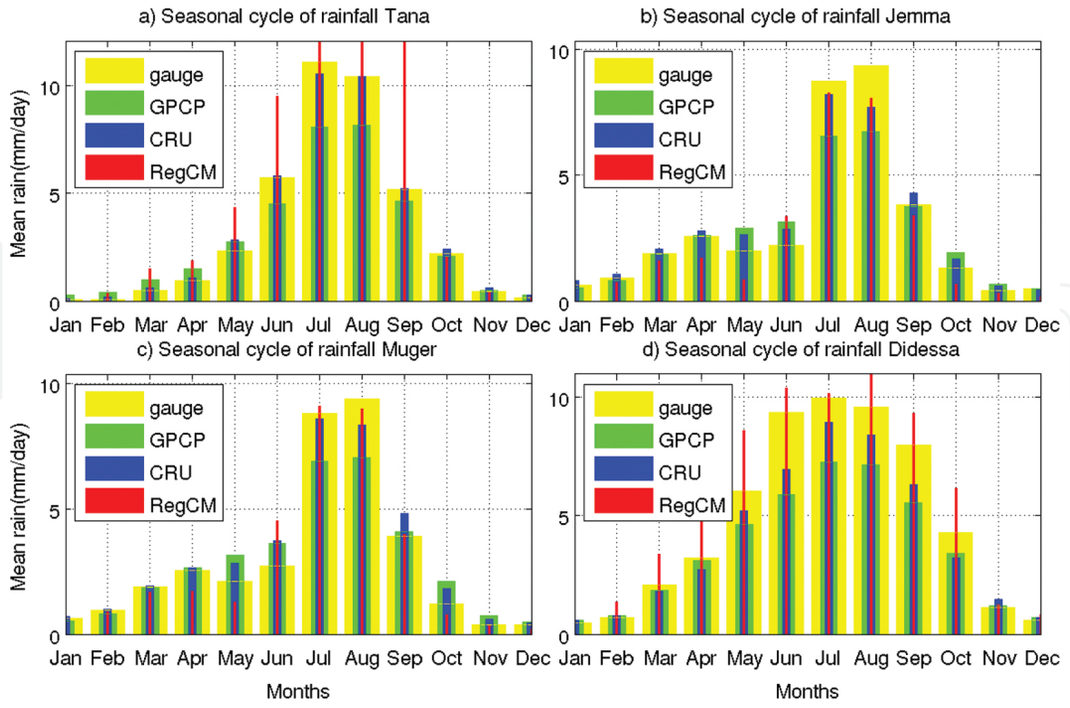

Figure 7. Areal averaged of homogeneous regions seasonal rainfall or annual cycle.

For Jemma and Muger regions (**Figure 7b** and **7c**), gauge, GPCP and CRU observations exhibit a maximum July–August and small rain during spring season. The model captures this cycle except small underestimation of the rainfall amount (compared to observational dataset or gauge). The Didessa region of the basin (**Figure 7d**) shows unimodal, but longer rainy season almost throughout the year maximum between May and September. However, there is a wide spread in the magnitude and phase of the precipitation maxima across these datasets, with the gauge showing the largest magnitudes, GPCP the smallest and CRU some intermediate values. RegCM4 also captures well the long seasonality, and slightly overestimate precipitation amounts throughout the year. Overall, RegCM4 performs well in reproducing the seasonal cycle of precipitation in all regions, except for an overestimation over the southwestern and central regions, where the rainfalls in almost all months is systematically underestimate over the eastern regions. We note that GPCP had better agreement in the magnitude, and especially, the phase of the rainy season peaks and corresponding breaks than CRU with respect to gauge dataset. Most previous studies of RegCM3 using a smaller domain centered over eastern Africa found difficulties to correctly reproduce the precipitation patterns. For example, in [18] performed 18 years of simulation with RegCM3 over eastern Africa and reported overestimation by >26% precipitation in Ethiopia, using the Grell/Emanuel convective scheme. In reference [8] indicated some deficiencies in capturing short east Africa rainy season of the observed rainfall over the Kenya Highlands and Lake Victoria Basin using RegCM3. Sun et al. [4] showed also some deficiencies over the Congo–Angola Basin and Kenya Highlands and the monsoon flow during the same period was stronger than observed.

Figure 8 shows the spatial patterns of correlation coefficient between the first dominant summer RPC1 of observational rainfall and the corresponding raw summer mean rainfall time

http://dx.doi.org/10.5772/64954

series at each grid point over the basin region. According to the result, the northeastern regions have high coefficient of variation in rainfall during summer season. The variance explained over this region is ~15, ~26, ~13 and ~33% of the total variance using gauges, GPCP, RegCM4 and CRU, respectively. The pattern of gauge (**Figure 8a**) is narrower when we compare with respect to GPCP and CRU and similar with model simulation (**Figure 8a**, **8b**, **8c** and **8d**). The model and gauge shows significant negative correlation over small western regions of the basin, unlike gauge and CRU. The corresponding RPC1 of RegCM4 significantly correlated with RPC1 of gauge (correlation between RPC1s of gauge and RegCM4 is ~0.67). Similarly, RegCM4-RPC1 correlated significantly with GPCP-RPC1 (correlation between them is ~0.82) and the two observational RPCs (gauge and GPCP) correlated with a magnitude of ~0.88. The dominant RPC of RegCM4 captured correctly the extreme positive years (e.g. 1983, 1989 and 1990) and extreme negative years (e.g., 1984, 2000 and 2008/2009) with that of corresponding observational RPCs.

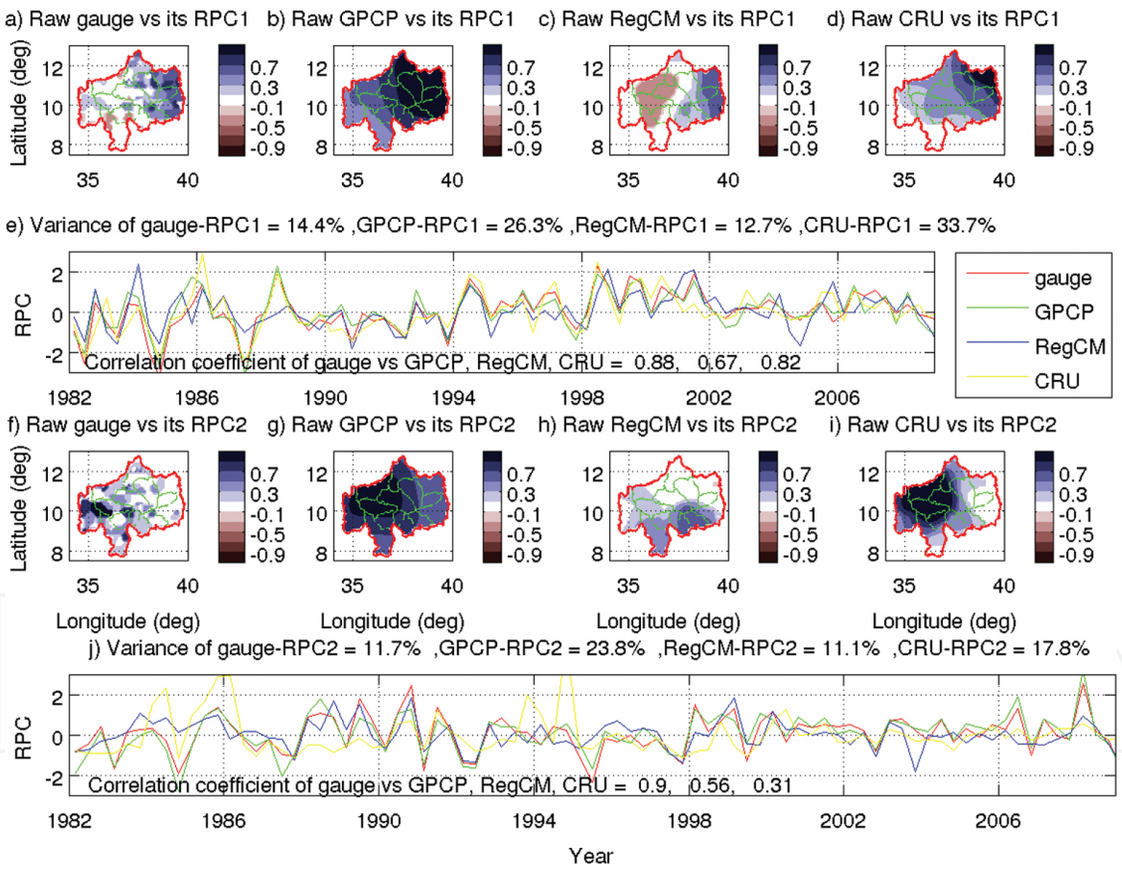

Figure 8. Summer season, correlation patterns of rainfall first dominant RPC1 with raw rainfall: (a) gauge, (b) GPCP, (c) RegCM, (d) CRU, (e) the time series of the RPC1 for the observations and the RCM, (f–i) correlation patterns of rainfall RPC2 with raw rainfall, of gauge, GPCP, RegCM and CRU, respectively and (j) the time series of the RPC2 for the observations and the RCM.

The second patterns of correlation between second RPC2 of rainfall and summer mean rainfall by gauge, GPCP and RegCM4 are shown in **Figure 8f**, **8g** and **8h**, respectively. The patterns in

all dataset indicate a strong correlation over northwestern and western regions of Upper Blue Nile River Basin. About 12, ~24 and ~11% variances are explained by the patterns out of total variance over southwestern region using gauge, GPCP and RegCM4, respectively. The variance explained by RegCM4 over this region is smaller than GPCP, but relatively same compared to gauge. RegCM4 and gauge RPC2 negatively correlated with their corresponding rainfall over northeastern region unlike GPCP. The second gauge RPC is significantly correlated with GPCP and RegCM4, with a correlation with ~0.9 and ~0.56, respectively. Similar to the first RPC, the observational RPC2 extreme positive years (e.g., 1983, 1988, 1996 and 2007) and extreme negative years (e.g., 1996, 2002, and 2008/9) are clearly reproduced by the model. Our simulation showed relatively good performance when we apply dry Grell over land and Emanuel over Ocean and we used ERA-Interim at the lateral boundaries of the simulation.

Observed areal averaged standardized anomalies of each homogeneous spring mean rainfall (not shown here) time series are significantly (a significance level of 95%) correlated with the corresponding simulation dataset. The result indicates the model standardized precipitation anomaly is highly correlated with the corresponding gauge and GPCP datasets. On the contrary, weak correlation over most of homogeneous regions with CRU dataset, which may be because of high spatial difference over the region, using small number of stations may bring such result between simulation and CRU dataset unlike GPCP and gauge. Similar results were reported by Tsidu [41].

Overall the RegCM4 simulates fairly the observed multi-scale spatial and inter-/intra-annual temporal variability of climate in UBNRBR (correlation with gauge >0.7). We also noticed GPCP represents the observed multi-scale variability better (correlation with gauge >0.83) than CRU for both homogeneous areal mean standardized time series and dominant RPCs.

4. Summary and conclusion

In this study, we investigated the ability of the RegCM4 to simulate the multi-scale spatial and temporal variability of large-scale circulation and rainfall for spring and summer season. The main large-scale circulation that connected with the generation of rainfall during summer season over the basin (such as TEJ and EALLJ) is realistically simulated. Comparison of ERA-Interim and RegCM4 horizontal upper level winds indicates a strong similarity in representing the location and strength of the TEJ core, even though the jet stream is slightly stronger in the model over regions of south Chad, Central African Republic, central and eastern Ethiopia. Model simulated low-level horizontal wind has a good agreement during summer season with reanalysis wind dataset in both the magnitude and direction over Ethiopia in general and the basin in particular. The correlation with simulated and ERA-Interim first dominant rotated principal components (~0.95) of upper level horizontal winds of summer is significant and high in magnitude. We also notice that similar patterns of RPC1s show the ability of the model to capture the features of this wind, which is highly connected with the rainfall variability over most of Upper Blue Nile basin regions during summer season. The low-level horizontal wind spatial patterns of dominant variability and high magnitude (correlation value of ~0.86) of the

http://dx.doi.org/10.5772/64954

corresponding RPCs also confirm the performance of the model to capture the main features of rain generating mechanisms over the basin.

Upper Blue Nile River Basin summer climate variability from different observation datasets along with the performance of the regional climate model (RegCM4) in reproducing this variability is also assessed. The observed rainfall datasets have indicated that central mountainous regions, S. Gojjam, Beles, Wonbera, Anger, southern of Dabus, Didessa and Tana basin receive on average more than 12 mm/day of rainfall during the summer season, on the contrary Beshilo, Welaka, and Jemma regions, which are semiarid, receive comparably less precipitation during this season. Similar climatological pattern of rainfall is shown using GPCP, although with positive and negative biases over the western mountainous regions and some isolated lowland areas, respectively.

The mean annual cycle for the homogeneous rainfall regions using different sets of observations (gauge, GPCP and CRU) and RegCM4 simulation shows RegCM4 performs well in reproducing the seasonal cycle of precipitation over all regions, except for an overestimation over the southwestern regions, where the rainfalls in almost all months and systematically underestimate the eastern regions. We have noted that GPCP had better agreement in magnitude, and especially, the phase of the rainy season peaks and corresponding breaks than CRU with respect to gauge dataset.

The correlation coefficients between simulated and observed rainfall anomalies normalized by the standard deviation over the 14 climate subregions during spring and summer seasons and between the first two dominant RPCs show the ability of RegCM4 simulation to reproduce intra-annual variability of rainfall over subregions of the basin. The first dominant pattern of observational dataset which explains the east and western regions for spring and summer seasons, respectively, is captured correctly by RegCM4 simulation with corresponding RPCs significant correlation (correlation >0.6). Similarly, the second dominant variability regions (spring-eastern and summer-western) are simulated fairly with significant correlation with corresponding RPCs (correlation >0.56) including extreme years.

The simulated climatologies and intra-annual variability of different homogeneous climate subregions of the basin are consistent with the observed variables in representing these subregions. In particular, the model reasonably reproduces the observed rainfall and wind field climatology and intra-annual variability during both seasons. Conversely, the model has evidently weak representation of variability of temperature during both seasons with respect to station and CRU temperatures and better with respect to ERA-Interim. The spatial and temporal characteristics of climate in the region of the Upper Blue Nile Basin have been presented. Rainfall is highly seasonal, roughly highest percent of annual rainfall occurring between June and September.

The model captures the general patterns of the observed rainfall distributions, in particular the ICTZ position and intensities, although it is overestimated by the model as compared to the observation datasets. Both gauge and GPCP show the highest correlations with regard to the two dominant RPCs as compared to the rest of the datasets, but the pattern of variability of the model is best agreed with the gauge intra-annual variability in both summer and spring

seasons. The RegCM4, compared to the observations, shows a little more bias in rainfall estimation than temperature. This shows that temperature variability depends more on local process, hence RegCM4 correct the temperature and make it to have better representation of observed variability.

Acknowledgements

The author like to acknowledge greatly National Meteorological Services of Ethiopia. The authors would like to thank NOAA/OAR/ESRL for providing the GPCP data via Web site at http://www.esrl.noaa.gov/psd/, ECMWF for providing the ERA-Interim dataset. The SST data are available from the National Ocean and Atmosphere Administration website at http://www.cdc.noaa.gov. The author would also like to extend his gratitude to Blue Nile Water Institute (BNWI) and David Tadesse for financial support to complete this work.

Author details

Tadesse Terefe Zeleke[1*], Baylie Damtie Yeshita[2] and Fentahun Muluneh Agidew[2]

*Address all correspondence to: tadessekid@yahoo.com

1 Blue Nile Water Institute, Bahir Dar University, Bahir Dar, Ethiopia

2 Washera Geospace and Radar Science Laboratory, Bahir Dar University, Bahir Dar, Ethiopia

References

[1] Giorgi F, Mearns L. Introduction to special section. Regional climate modeling revisited. J Geophys Res. 1999; 104:6335–6352.

[2] Giorgi F, Shields C. Tests of precipitation parameterizations available in latest version of NCAR regional climate model (RegCM) over continental United States. J Geophys Res. 1999; 104(D6):6353–6375.

[3] Small EE, Giorgi F, Sloan LC. Regional climate model simulation of precipitation in central Asia: mean and interannual variability. J Geophys Res. 1999; 104:6563–6582.

[4] Sun L, Semazzi F, Giorgi F, Ogallo LA. Application of the NCAR regional climate model to eastern Africa. Part I: simulation of the short rains of 1988. J Geophys Res. 1999a; 104:6529-6548.

[5] Sun L, Semazzi F, Giorgi F, Ogallo LA. Application of the NCAR regional climate model to eastern Africa. Part II: simulation of interannual variability of short rains. J Geophys Res. 1999b;104:6549–6562.

[6] Wang Y, Leung LR, McGregor JL, Lee DK, Wang WC, Ding Y, Kimura F. Regional climate modeling: progress, challenges and prospects. J Meteorol Soc Jpn. 2004; 82:1599–1628.

[7] Pal JS, Giorgi F, Bi X, Elguindi N, Solomon F, Gao X, Francisco R, Zakey A, Winter J, Ashfaq M, Syed F, Bell JL, Diffanbaugh NS, Kamacharya J, Konare A, Martinez D, da Rocha RP, Sloan LC, Steiner A. The ICTP RegCM3 and RegCNET:regional climate modeling for the developing world. Bull Am Meteorol Soc. 2007; 88:1395–1409.

[8] Anyah RO, Semazzi F. Variability of East African rainfall based on multiyear RegCM3 simulations. Inter J Climatol. 2007; 27:357–371.

[9] Dickinson RE, Errico RM, Giorgi F, Bates GT. A regional climate model for the western United States. Clim Change. 1989; 15:383-422.

[10] Giorgi F, Bates GT. The climatological skill of a regional model over complex terrain. Mon Wea Rev 1989; 117:2325–2347.

[11] Giorgi F, Bates GT, Nieman SJ. The multi-year surface climatology of a regional atmospheric model over the western United States. J Clim. 1993a; 6:75–95.

[12] Giorgi F, Marinucci MR, Bates GT. Development of a second generation regional climate model (RegCM2). I: boundary layer and radiative transfer processes. Mon Weather Rev. 1993b; 121:2794–2813.

[13] Denis B, Laprise R, Cˆotˆe J. Donwscaling ability of one-way nested regional climate models: the big-brother experiment. Climate Dynamics. 2002; 18:627–646.

[14] Leung LR, Ghan SJ. Pacific Northwest climate sensitivity simulated by a regional climate model driven by a GCM. Part I: control simulation. J Clim. 1999; 12:2010–2030.

[15] Giorgi F. Simulation of regional climate using a limited area model nested in a general circulation model. J Clim. 1990; 3:941–963.

[16] Giorgi F, Bi X. A study of internal variability of a regional, climate model. J Geophys Res. 2000; 105(D24):29503–29521.

[17] Davis N, Bowden J, Semazzi F, Xie L, Onol B. Customization of RegCM3 regional climate model for eastern Africa and a tropical Indian Ocean domain. J Clim. 2009; 22:3595–3616. doi:10.1175/2009JCLI2388-1.

[18] Segele ZT, Leslie LM, Lamb PJ. Evaluation and adaptation of a regional climate model for the Horn of Africa: rainfall climatology and interannual variability. Inter J Climatol. 2008; 29(1), 47–65 doi:10.1002/joc.1681.

[19] Zeleke T, Giorgi F, Mengistu Tidu G, Diro GT. Spatial and temporal variability of summer rainfall over Ethiopia from observations and a regional climate model experiments. Theor Appl Climatol. 2013; 111:665–681. doi 10.1007/s00704-012-0700-4.

[20] Giorgi F, Coppola E, Solmon F, Mariotti L, Sylla MB, Bi X, Elguindi N, Diro GT, Nair V, Giuliani G, Turuncoglu UU, Cozzini S, Guettler I, O'Brien TA, Tawfik AB, Shalaby A, Zakey AS, Steiner AL, Stordal F, Sloan LC, Brankovic C. RegCM4: model description and preliminary tests over multiple CORDEX domains. Clim Res. 2012; 52:7–29.

[21] Grell GA, Dudhia J, Stauffer DR. Description of the fifth generation Penn State/NCAR mesoscale model (MM5). Technical note. 1994; 121p. NCAR/TN-398-STR.

[22] Kiehl JT, Hack JJ, Bonan GB, Boville BA, Briegleb BP, Williamson DL, Rasch PJ. Description of the NCAR community climate model (CCM3). Technical Report. 1996;152p. TN-420-STR. NCAR, Boulder.

[23] Holtslag AAM, DeBruin EIF, Pan HL. A high resolution air mass transformation model for short-range weather forecasting. Mon Weather Rev. 1990; 118:1561–1575.

[24] Dickinson RE, Henderson SA, Kennedy PJ. Biosphere-Atmosphere Transfer Scheme (BATS) version 1E as coupled to the NCAR Community Climate Model. Technical Note. 1993;72p. NCAR/TN-387 + STR.

[25] Pal JS, Small EE, Eltahir EAB. Simulation of regional-scale water and energy budgets: representation of sub-grid cloud and precipitation processes within RegCM. J Geophys Res. 2000; 105:29579–29594.

[26] Anthes RA. A cumulus parameterization scheme utilizing a one dimensional cloud model. Mon Weather Rev. 1977; 105:270–286.

[27] Emanuel KA, Rothman MZ. Development and evaluation of a convection scheme for use in climate models. J Atmos Sci. 1999; 56:1756–1782.

[28] Fritsch JM, Chappell CF. Numerical prediction of convectively driven mesoscale pressure systems. Part I: convective parameterization. J Atmos Sci. 1980; 37:1722–1733.

[29] Dee DP, Uppala SM, Simmons AJ, Berrisford P, Poli P, Kobayashi S, Andrae U, Balmaseda MA, Balsamo G, Bauer P, Bechtold P, Beljaars A, van de Berg L, Bidlot J, Bormann N, Delsol C, Dragani R, Fuentes M, Geer AJ, Haimberger L, Healy SB, Hersbach H, Hólm EV, Isaksen L, Kållberg P, Köhler M, Matricardi M, McNally AP, Monge-Sanz BM, Morcrette JJ, Park BK, Peubey C, de Rosnay P, Tavolato C, Thépaut JN, Vitart F. The ERA-Interim reanalysis: configuration and performance of the data assimilation system. Q J R Meteorol Soc. 2011; 137:553–597. doi:10.1002/qj.828.

[30] Reynolds RW, Rayner NA, Smith TM, Stokes DC, Wang W. An improved in situ and satellite SST analysis for climate. J Clim. 2002; 15:1609–1625.

[31] Zeleke T, Giorgi F, Mengistu Tidu G, Diro GT. Spatial and temporal variability of summer rainfall over Ethiopia from observations and a regional climate model experiments. Theor Appl Climatol. 2013. doi:10.1007/s00704-012-0700-4.

[32] Adler RF, Huffman GJ, Chang A, Ferraro R, Xie P, Janowiak J, Rudolf B, Schneider U, Curtis S, Bolvin D, Gruber A, Susskind J, Arkin P. The Version 2 Global Precipitation Climatology Project (GPCP) monthly precipitation analysis (1979–present). J Hydrometeorol. 2003; 4:1147–1167.

[33] Rayner NA, Brohan P, Parker DE, Folland CK, Kennedy JJ, Vanicek M, Ansell TJ, Tett SFB: Improved analyses of changes and uncertainties in sea surface temperature measured in situ since the mid-nineteenth century: The HadSST2 Dataset. J Clim. 2006; 19:446–469. doi:10.1175/JCLI3637.1.

[34] Kistler R, Kalnay E, Collins W, Saha S, White G, Woollen J, Chelliah M, Ebisuzaki W, Kanamitsu M, Kousky V, Dool H, Jenne R, Fiorino M. The NCEP-NCAR 50-year reanalysis: monthly means CD-ROM and documentation. Bull Am Meteor Soc. 2001; 82:247–268.

[35] Navarra A, Simoncini V. A guide to empirical orthogonal functions for climate data analysis. Springer: Dordrecht; 2010. doi:10.1007/978-90-481-3702-21.

[36] Richman MB. Rotation of principal components. J Climatol. 1986; 6:293–335.

[37] Jolliffe IT. Rotation of principal components: some comments. J Climatol. 1987; 7:507–510. doi:10.1002/joc.3370070506.

[38] Rencher AC. Multivariate statistical inference and applications. Wiley: New York; 1998.

[39] Von Storch H, Zwiers FW. Statistical analysis in climate research. Cambridge University Press. 1999; 484 p. ISBN 0521 450713.

[40] Camberlin P, Philippon N. The East African March-May Rainy season: Associated Atmospheric dynamics and predictability over the 1968-97 periods. J Clim. 2002; 15:1002–1019.

[41] Tsidu M. High-resolution monthly rainfall database for Ethiopia: homogenization, reconstruction, and gridding. J Clim. 2012; 25:8422–8443.

IntechOpen